

Article

# Formulation of Piperine Ternary Inclusion Complex Using $\beta$ CD and HPMC: Physicochemical Characterization, Molecular Docking, and Antimicrobial Testing

Sultan Alshehri <sup>1,2</sup> , Syed Sarim Imam <sup>1,\*</sup> , Afzal Hussain <sup>1</sup>  and Mohammad A. Altamimi <sup>1</sup>

<sup>1</sup> Department of Pharmaceutics, College of Pharmacy, King Saud University, Riyadh 11451, Saudi Arabia; salshehri1@ksu.edu.sa (S.A.); amohammed2@ksu.edu.sa (A.H.); maltamimi@ksu.edu.sa (M.A.A.)

<sup>2</sup> College of Pharmacy, Almareefa University, Riyadh 13713, Saudi Arabia

\* Correspondence: simam@ksu.edu.sa or sarimimam@gmail.com

Received: 5 October 2020; Accepted: 10 November 2020; Published: 12 November 2020



**Abstract:** The present study was designed to evaluate the effect of hydroxyl propyl methyl cellulose (HPMC) on the complexation efficiency and dissolution of piperine (PPR) and  $\beta$  cyclodextrin ( $\beta$  CD) complex. The binary and ternary inclusion complexes were prepared using solvent evaporation and microwave irradiation methods. The samples were further evaluated for physicochemical evaluation, morphology, antimicrobial, and antioxidant activities. The binary and ternary samples showed high stability constant (Ks) value and complexation efficiency (CE). The dissolution study results revealed marked enhancement in the release of the binary inclusion complex and ternary inclusion complex compared to pure PPR. Fourier transform infrared (FTIR), nuclear magnetic resonance (NMR), and molecular docking results confirm the complex formation. X-ray powder diffractometry (XRD) and scanning electron microscopy (SEM) data revealed modification in the structure of PPR. 2,2-diphenyl-1-picrylhydrazyl (DPPH) scavenging and antimicrobial results showed enhanced activity in the PPR complex in comparison to pure PPR. In conclusion, a remarkable enhancement in dissolution, antioxidant and antimicrobial activities were attained due to marked improvement in solubility through complexation of PPR with HPMC/ $\beta$  CD.

**Keywords:** piperine;  $\beta$  CD; HPMC; inclusion complex; anti-oxidant; antimicrobial; molecular docking

## 1. Introduction

The formulation design of a potent drug delivery system is very critical for pharmaceutical applications. There are a number of biodegradable and biocompatible drug carriers that have been developed in the last decades with enhanced therapeutic potential. There were many applications of the cyclodextrin (CDs) complex as an effective method for the enhancement of solubility and dissolution of water insoluble drugs [1–4].

CDs are cyclic oligosaccharides consisting of  $\alpha$ -1,4-glycoside linkages and the three different types of CDs are recognized as  $\alpha$  CD (six D-glucose units),  $\beta$  CD (seven D-glucose units), and  $\gamma$  CD (eight D-glucose units). The presence of 1° and 2° hydroxyl groups at the outer surface of CDs make them hydrophilic in nature from the outside and hydrophobic from the inner side. Among the three CDs,  $\beta$  CD (Figure 1A) is the most commonly used CD in the formulation design due to its big size cavity, minimal to no toxicity, and biodegradability [5,6]. The truncated cone shape structure of  $\beta$  CD helps to form the inclusion complex with the hydrophobic molecule through non covalent interaction without any chemical reaction [7]. Recently, the complexation efficiency of insoluble drugs has been enhanced with the addition of a small quantity of auxiliary substances like hydrophilic polymers, hydroxyl acids,

and surfactant as complexation media to form ternary complexes [8,9]. The use of ternary substance in the binary complex gives a supramolecular stable ternary system. The ternary system may help to achieve better physicochemical properties of drugs in comparison to the binary system [10].

Piperine (PPR, Figure 1B) is a crystalline alkaloid obtained from black pepper, long pepper, and other pepper species. The chemical name of PPR is (E,E)-1-piperoylpiperidine and (E,E)-1-[5-(1,3-benzodioxol-5-yl)-1-oxo-2,4-pentdienyl] piperidine. The water solubility of PPR is (40 µg/mL) [6], and its melting point is 135 °C. PPR has a wide range of pharmacological activities, including antioxidant, anti-inflammatory, antiarthritic, anticancer, antifungal, and antimicrobial [11,12]. PPR has been reported for insecticidal activity against third star larvae of *C. pipiens pallens*, *A. aegypti*, and *A. togoi* [13]. It has shown the antibacterial concentration between 100–500 µg/mL against *S. aureus*, *P. aeruginosa*, *B. subtilis*, and *E. coli* [13,14]. In spite of the valuable therapeutic efficacy, their application in the delivery system is limited due to poor water solubility and bioavailability [12,15].

In our literature survey, there is no research report published about the ternary inclusion complex of PIP with  $\beta$  CD:HPMC (Figure 1C). The present study was designed to investigate the effect of co-complexing agent (hydrophilic polymer: HPMC) on the PPR  $\beta$  CD inclusion complex. The phase solubility study was performed for the binary complex (PPR: $\beta$  CD) as well as the ternary complex (PPR: $\beta$  CD:HPMC) to check the effect of HPMC on complexation efficiency. The complex was prepared by two different methods, like solvent evaporation (SE) and microwave irradiation (MI) methods. The comparative solubility and dissolution study between the binary inclusion complex and ternary inclusion complex was performed to check the effect of ternary substance (HPMC). The prepared samples were further characterized by FTIR, SEM, XRD, NMR ( $^1\text{H}$  and  $^{13}\text{C}$ ), and molecular docking. Finally, the selected system was evaluated for antioxidant and antimicrobial activity to check the effect of the prepared inclusion complex.

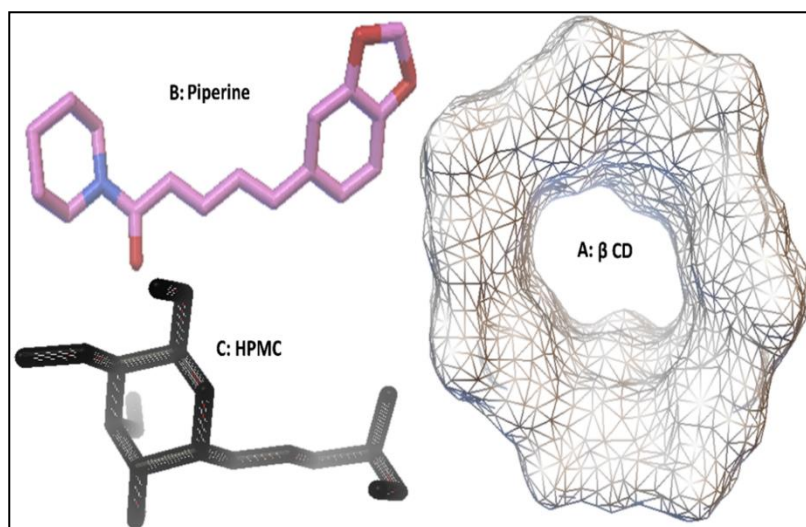


**Figure 1.** Chemical structure of (A) beta cyclodextrin, (B) piperine, (C) hydroxy propyl methyl cellulose.

## 2. Material and Methods

### 2.1. Material

Piperine (PPR) was procured from “Beijing Mesochem Technology Co. Pvt. Ltd. (Beijing, China)”. Beta cyclodextrin (HP  $\beta$  CD) was obtained from Sigma, Steinheim, Germany. Hydroxy propyl methyl cellulose (HPMC) was purchased from Alfa Aesar, Ward Hill, MA, USA. All other chemicals used were of analytical grade. Milli Q water was collected from the purification unit and used for the study. *S. aureus*, (ATCC-29213), *B. subtilis* (ATCC-10400), *E. coli* (ATCC-25922), *E. faecalis* (ATCC 29212), were obtained from the Department of Microbiology, College of Pharmacy, King Saud University Riyadh, Saudi Arabia.

## 2.2. Methods

### 2.2.1. Phase Solubility Study

The phase solubility study was evaluated to check the stability constant and complexation efficiency of the binary and ternary composition. The study was performed as per the reported procedure of Higuchi and Connors [16]. The aqueous solution of  $\beta$  CD (0–10 mM) and  $\beta$  CD (0–10 mM) with HPMC (5%) was prepared and an excess amount of PPR was added [17]. The prepared suspension was kept on an orbital shaker at room temperature (25 °C) for 72 h. After that, the samples were collected, filtered (0.45  $\mu$ m), and assayed using a UV spectrophotometer (Jasco V 530, Hachioji, Tokyo, Japan) at 341 nm. The stability constant ( $K_s$ ) and complexation efficiency (CE) were calculated for each sample using the slope of phase solubility graph:

$$K_s = \frac{\text{slope}}{S_0 (1 - \text{slope})} \quad (1)$$

where  $S_0$  = PPR solubility without additives.

The complexation efficiency (CE) was also calculated using the below formula:

$$CE = \frac{\text{slope}}{1 - \text{slope}} \quad (2)$$

### 2.2.2. Formulation of Inclusion Complex

The two different formulations (piperine binary inclusion complex (PPR BC) and piperine ternary inclusion complex (PPR TC)) were prepared by two different methods like solvent evaporation (SE) and the microwave irradiation (MI) method. The composition of the binary complex prepared with PPR- $\beta$  CD and the ternary complex prepared with PPR- $\beta$  CD-HPMC in a fixed ratio is shown in Table 1.

**Table 1.** Formulation design of the piperine inclusion complex using different methods (*w/w*).

Piperine Binary Complex			Piperine Ternary Complex		
Physical Mixture	Solvent Evaporation	Microwave Irradiation	Physical Mixture	Solvent Evaporation	Microwave Irradiation
PPR: $\beta$ CD	PPR: $\beta$ CD	PPR: $\beta$ CD	PPR: $\beta$ CD: HPMC *	PPR: $\beta$ CD: HPMC *	PPR: $\beta$ CD: HPMC *
1:1	1:1	1:1	1:1	1:1	1:1

\* 5% *w/w* concentration of HPMC added in ternary complex, (*w*—weight).

### 2.2.3. Physical Mixture

The binary complex (PPR- $\beta$  CD) and ternary complex (PPR- $\beta$  CD-HPMC) were prepared by geometric mixing of each component. Each sample was weighed accurately, mixed, and triturated in a mortar and pestle. Finally, the samples were sieved through a mesh and kept in a desiccator for further evaluation.

### 2.2.4. Solvent Evaporation Method

The binary and ternary inclusion complexes were prepared by taking the weighed quantity of each ingredients and dissolved in a solvent blend of ethanol (96% *v/v*) and water (3:7). The solvent was completely evaporated until a dried mass was prepared. Then, the samples were kept in a vacuum oven at a temperature of 50 °C for 48 h for the complete removal of solvents [18]. Finally, the dried samples were pulverized to make powder, and passed through a sieve to get uniform fine particles. The prepared samples were stored in a desiccator for further characterization.

### 2.2.5. Microwave Method

In this method, the weighed samples for binary and ternary inclusion complexes were taken. The binary complex prepared with the PPR- $\beta$  CD blend is in a fixed ratio. The samples were taken in a small beaker and homogenous paste was prepared with the addition of a solvent blend of ethanol (96% *v/v*) and water (3:7). The prepared samples were kept in a microwave oven (Samsung ME0113M1, Kuala Lumpur, Malaysia) and irradiated at 500 W for 5 min. The same procedure is followed to prepare the ternary inclusion complex with the addition of HPMC as an auxiliary substance. The ternary sample was irradiated for 4 min at the same temperature and power. Finally, the samples were collected, kept aside for cooling, then milled and sieved through a mesh (#80) to get uniform size particles. The samples were stored in a desiccator for further characterization.

### 2.2.6. Dissolution Study

The release study was performed for the prepared binary and ternary inclusion complexes to check the difference in the release profile. The study was performed in the dissolution apparatus with the paddle method using 900 mL release media (phosphate buffer, pH 7.4) at a temperature of  $37 \pm 0.5$  °C with 50 rpm [19]. Each sample containing (~15 mg of PPR) were placed in the release media and at a specific time interval, the released sample (5 mL) was removed from the vessel. The same volume of fresh release media was replaced to maintain the volume. The released content at each time point was assessed by using a UV spectrophotometer.

### 2.2.7. X-ray Diffraction

X-ray diffraction study was used to evaluate the changes in the diffraction pattern of pure PPR after complexation with cyclodextrin by the solvent evaporation and microwave irradiation method. The changes in the peak size and symmetry was evaluated by comparing the XRD spectra of PPR TPM, PPR TCM, PPR TCS with the pure PPR. The study was performed on the diffractometer (Ultima IV, Rigaku Inc. Tokyo, Japan) with a scanning rate of 0.5°/min in the scanning range of 3° to 60°. The characteristic peak of each sample was assessed by collecting the data by monochromatic radiation (Cu K $\alpha$ 1,  $\lambda = 1.54$  Å), operating at a voltage of 40 kV and current of 40 mA.

### 2.2.8. Surface Morphology

Scanning electron microscope was used to compare the surface morphology of the different samples of pure PPR, PPR TPM, PPR TCM, and PPR TCS. The study was performed by using the electron microscope (JSM 6360A, JOEL, Tokyo, Japan). The samples were coated with gold and observed under the microscope at high resolution to check the change in morphology.

### 2.2.9. Fourier Transform Infrared (FTIR)

The formation of the complex was assessed by evaluating the change in peak shape, position, and intensity. The spectra of PPR,  $\beta$  CD, HPMC, PPR TPM, PPR TCM, and PPR TCS were compared to interpret the spectra. The spectrophotometer (ATR-FTIR, Bruker, Alpha, Ettlingen, Germany) was used to study the samples. The analysis was performed between 4000–400  $\text{cm}^{-1}$  and the conformational changes were observed.

### 2.2.10. Nuclear Magnetic Resonance (NMR)

NMR study was used to check the formation of the complex and the conformational changes in the prepared PPR TPM, PPR TCM, and PPR TCS with the pure PPR and  $\beta$  CD. The study was performed with the spectroscopy (Bruker NMR, Fällanden, Switzerland; software topspin 3.2) and  $^1\text{H}$  NMR was performed at 700 MHz and  $^{13}\text{C}$  125 MHz, respectively. Each sample was prepared in deuterated DMSO and TMS used as an internal standard.

### 2.2.11. Antioxidant Activity

The antioxidant activity of the pure PPR, PPR TCM, and PPR TCS was performed as per the reported procedure with some modifications [20]. The stock solution (10 mg/mL) for all samples was prepared in ethanol. The samples were diluted further with ethanol to make a concentration of 100 µg/mL. The DPPH solution (0.02%) was separately prepared in ethanol (96% v/v). The DPPH solution (125 µL) was taken and mixed well with each sample (1 mL). The samples were mixed together and kept in the dark for 30 min. The chemical reaction takes place between the DPPH solution to react with antioxidants present in the sample, and the change in color from violet to yellow takes place. The tested samples were evaluated at 517 nm and the blank sample was prepared without the addition of PPR and the antioxidant activity was calculated in triplicate using the equation:

$$\text{Radical Scavenging (\%)} = \frac{(A_c - A_t)}{A_c} \times 100, \quad (3)$$

where  $A_c$  = Control sample absorbance,  $A_t$  = Test sample absorbance.

### 2.2.12. Antimicrobial Study

The agar diffusion method was performed to evaluate the antimicrobial activity of the prepared samples (pure PPR, PPR TCM, and PPR TCS) [20]. The bacterial strains were sub-cultured in nutrient broth (NB) in specified incubation condition. The bacterial strains (*S. aureus*, *Bacillus subtilis*, *E. coli*, *E. faecalis*) were exponentially grown at an optical density (OD600) of 0.6 (absorbance at 600 nm). The bacterial strains were cultured in a nutrient broth for 24 h. The bacterial suspension (200 µL) was spread on Luria Broth agar and a 6 mm diameter well was prepared with the help of a sterilized steel borer. The samples (100 µL) were transferred to wells, and incubated for 24 h at  $37 \pm 1$  °C. Antibacterial activity was evaluated by measuring the zone of inhibition. Rifampicin and ciprofloxacin were used as a positive control in the study.

### 2.2.13. Molecular Docking Studies

The molecular docking study of piperine with  $\beta$ -cyclodextrin ( $\beta$  CD) in the presence of hydroxypropyl methylcellulose (HPMC) was carried out as a ternary complex using Easy Dock Vina 2.2 and Autodock 4.2. Using online SMILES Translator and Structure File Generator, PPR and HPMC ligand structures SMILES notation was prepared. The geometry optimization was done using Open Babel 2.4.1. The crystal structure of  $\beta$  CD crystal was retrieved and extracted from the PDB co-crystal of  $\beta$ -amylase (PDB code:1BFN, resolution-2.07 Å) [21]. Easy Dock Vina 2.2 software was used to generate docking results of ternary inclusion complex. Finally, the docking result of the ternary inclusion complex was represented on Autodock tools (ADT) version 1.5.6 ([www.autodock.scrips.edu](http://www.autodock.scrips.edu)) using Vina Result.

### 2.2.14. Statistical Analysis

Statistical analysis of the results was performed using the Graph Pad InStat 3 software (San Diego, CA, USA). The results were presented in mean  $\pm$ SD. The dissolution and antioxidant data were analyzed using the Dunnet test. When there was a statistically significant difference, significant level was set at  $p < 0.01$ .

## 3. Result and Discussion

### 3.1. Phase Solubility Study

The phase solubility study was performed to evaluate the stability constant and complexation efficiency. The phase solubility graph of the binary sample (PPR- $\beta$  CD) and ternary sample (PPR- $\beta$  CD-HPMC) are shown in Figure 2. The result of the study revealed a linear enhancement in PPR

solubility with increase in  $\beta$  CD concentration. The slope value of both the system was found closer to unity. The stoichiometric ratio (1:1) suggested by the result to form a complex between PPR and  $\beta$  CD [22]. The binary and ternary systems showed the stability constant ( $K_s$ ) value of  $287 \text{ M}^{-1}$ ,  $464 \text{ M}^{-1}$ , and complexation efficiency (CE) value 4.1 and 6.6, respectively. Similar types of findings were found in our previous published literature of the piperine inclusion complex using TPGS as a ternary substance. The ternary inclusion system showed higher stability constant ( $K_s$ ) value and complexation efficiency (CE) value. The higher stability constant value of the ternary system gives a more stable complex than the binary system [23]. The presence of the ternary substance in the binary system interacts with the outer surface of CDs and helps to form a co-complex or aggregates [24]. The stability constant value between  $100\text{--}1000 \text{ mol/L}$  was reported for the biological application. The value less than  $100 \text{ mol L}^{-1}$  gives an unstable complex and a value higher than  $1000 \text{ mol L}^{-1}$  affects the drug absorption [25].

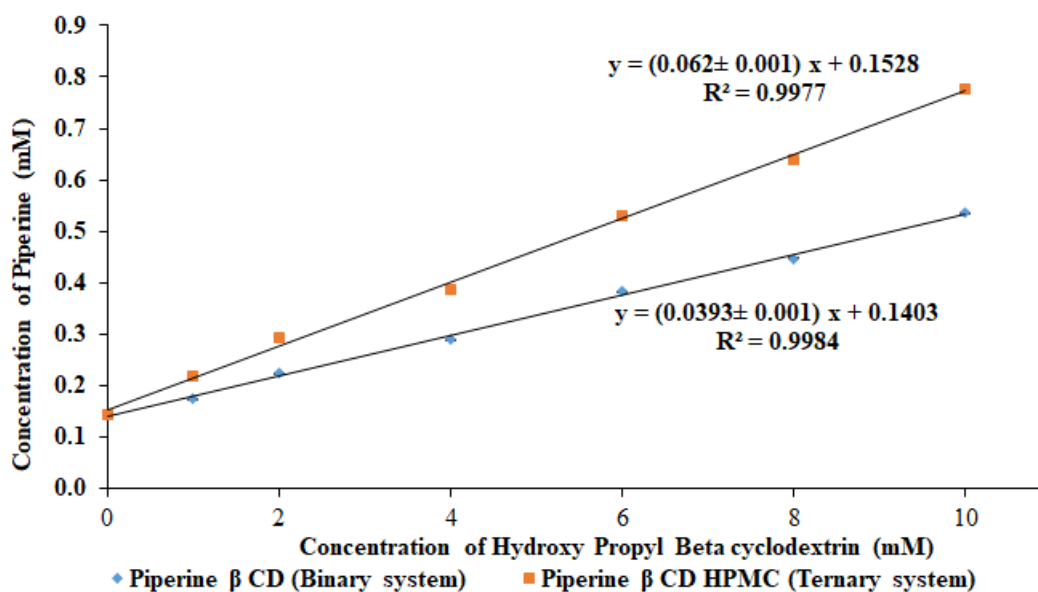


Figure 2. Phase solubility study of binary (PPR- $\beta$  CD) and ternary (PPR- $\beta$  CD-HPMC) samples.

### 3.2. Dissolution Study

The drug release study was performed and the comparative results are shown in Figure 3. The drug release data depicted a significant difference in release pattern from pure PPR (Table 2). The drug release profile followed the pattern as PPR TCM > PPR TCS > PPR TPM > PPR BCM > PPR BCS > PPR. The similar pattern was found in published literature [9,23,26]. The inclusion complex prepared by the microwave irradiation method showed a higher dissolution profile due to greater complexation efficiency. The ternary complex system (PPR TCM) showed about  $97.61 \pm 0.48\%$  release in the 60 min study and the PPR TCS system showed  $95.78 \pm 0.38\%$  PPR release in the same time. The pure PPR and TPM showed  $22.04 \pm 0.48\%$  (the release content was found to be very low in the studied time during the study due to poor solubility and initial points were found below the lower limit of quantification) and  $62.42 \pm 0.1\%$  drug release profile. The binary inclusion complex systems (PPR BCM and PPR BCS) released  $65.02 \pm 0.77\%$  and  $50.78 \pm 1.15\%$ . The binary complex systems also showed a significant difference in the release pattern than pure PPR. The enhancement in the PPR release was due to enhanced solubility of pure PPR by partial entrapment into the  $\beta$  CD complex [26]. The higher drug release was achieved due to enhanced PPR solubility in the inclusion complex. The ternary inclusion complex showed the maximum PPR release in 60 min, whereas at the same time, the binary inclusion complex showed a release profile between 50–65% only. The addition of HPMC as a ternary substance in the PPR- $\beta$  CD complex lead to significant ( $p < 0.01$ ) enhancement in the release. It helps in higher solubility, inclusion, and complexation of PPR [23].

The presence of two solubilizers ( $\beta$  CD and HPMC) in the ternary inclusion complex have shown synergistic effect on the drug solubilization. Both the solubilizers are available for PPR to act as a solubility enhancer by inclusion complexation [23,27]. A slight difference in the release pattern was also observed between the ternary inclusion complex (PPR TCS and PPR TCM). The sample prepared by the microwave irradiation method showed higher and faster release than the sample prepared with the solvent evaporation method. The application of microwave rays helps to produce a uniform heating rate to the test sample and also gives better intimate contact between drug and carrier [28,29].

**Table 2.** Comparative evaluation data of piperine and piperine formulations.

Samples	Release Study (%)	Antioxidant Study (%)	Antimicrobial Activity (in mm)			
			(ZOI Noted after Subtracting the Value of Well 6 mm)			
	(60 min)	(%)	<i>S. aureus</i>	<i>B. subtilis</i>	<i>E. coli</i>	<i>E. faecalis</i>
Pure PPR	22.04	38.92 $\pm$ 2.38	11.4 $\pm$ 0.45	9.3 $\pm$ 0.38	11.8 $\pm$ 0.65	6.9 $\pm$ 0.53
PPR TPM	62.42	59.42 $\pm$ 4.1	-	-	-	-
PPR TCS	95.78	72.37 $\pm$ 5.35	15.5 $\pm$ 0.89	13.1 $\pm$ 0.72	16.5 $\pm$ 0.66	11.3 $\pm$ 0.85
PPR TCM	97.61	79.19 $\pm$ 4.34	15.7 $\pm$ 0.73	12.9 $\pm$ 0.79	16.2 $\pm$ 0.82	11.9 $\pm$ 0.53

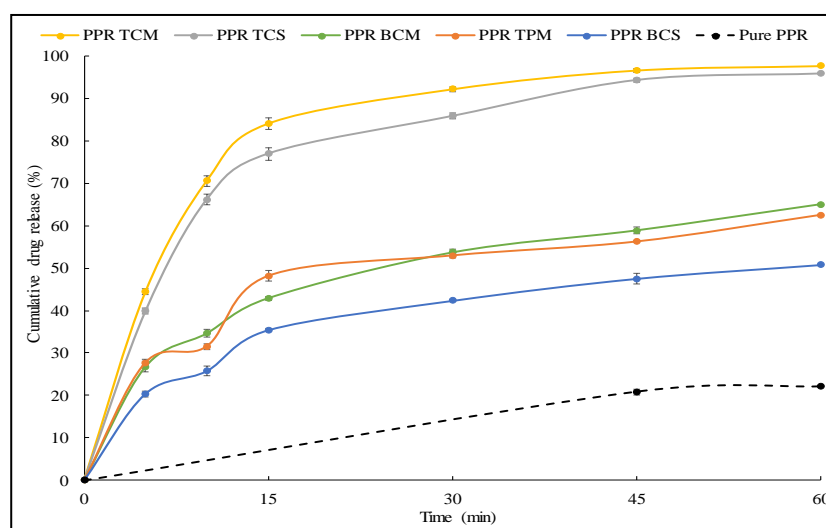


**Figure 3.** Comparative dissolution profile of pure piperine and piperine binary and ternary complexes. Values are presented as mean  $\pm$  SD with triplicates. (Dashed line indicates released value at 45 and 60 min.).

### 3.3. X-ray Diffraction

Changes in the nature of PPR were evaluated by the XRD study after complexation with  $\beta$  CD and HPMC and are shown in Figure 4. The comparison in peak height, peak intensity, and the peak shifting was performed to evaluate and check the changes in the crystalline nature of PPR. The characteristic peak of PPR was compared with the prepared samples (PPR TPM, PPR TCM, PPR TCS). The pure PPR thermogram showed the characteristic sharp intense characteristic diffraction angle between 10–30°. The sample PPR TPM showed the low intensity peaks due to the partial loss of crystallinity. However, in the sample of PPR TCM and PPR TCS, there were significant changes in the characteristic peak of PPR observed. The peak height and intensity are markedly reduced and converted to very low intensity peaks. Some peaks are fused and broadened as compared to the pure molecule. Marked changes were observed in the peaks due to complexation of pure PPR with  $\beta$  CD and HPMC. There was slight difference in the results of sample prepared by solvent evaporation and the microwave irradiation method. The sample prepared with the microwave method showed low intensity and broad peaks due to higher transformation of crystalline into amorphous PPR by microwave irradiation.

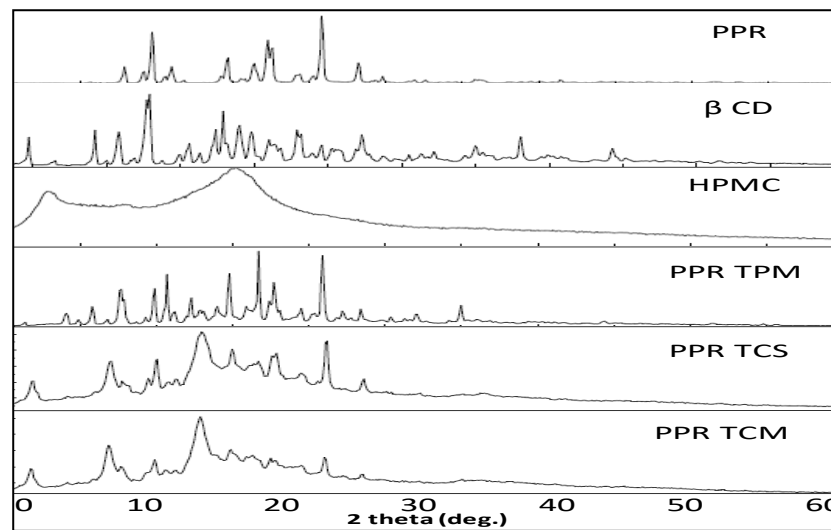


**Figure 4.** XRD images of pure samples (piperine,  $\beta$  CD, HPMC), piperine physical mixture (PPR TPM), piperine ternary inclusion complex (PPR TCM), piperine ternary inclusion complex (PPR TCS).

### 3.4. Surface Morphology

The surface morphology of the pure PPR and prepared samples was evaluated to check the changes in structure after formation of inclusion complex Figure 5. The sample of pure PPR showed the well-defined crystal structure. In the case of PPR TPM, there was a lesser amount of crystal structure of PPR observed. There are some amorphous agglomerates also observed due to close contact of  $\beta$  CD and HPMC. The samples prepared by solvent evaporation (PPR TCS) and the microwave irradiation (PPR TCM) method showed more amorphous and homogenous structure with the porous surface. The preparation methods and the presence of complexing agent  $\beta$  CD and HPMC were significantly able to transform the crystalline structure into an amorphous one. The change in particles shape and aspect in the inclusion confirms the formation of the new solid phase due to habitus change upon complexation [23,30]. The formation of the amorphous structure was confirmed by XRD and dissolution study. There was greater and faster solubility observed with the amorphous material due to the high internal energy and molecular motion as compared to the crystalline structure [31].

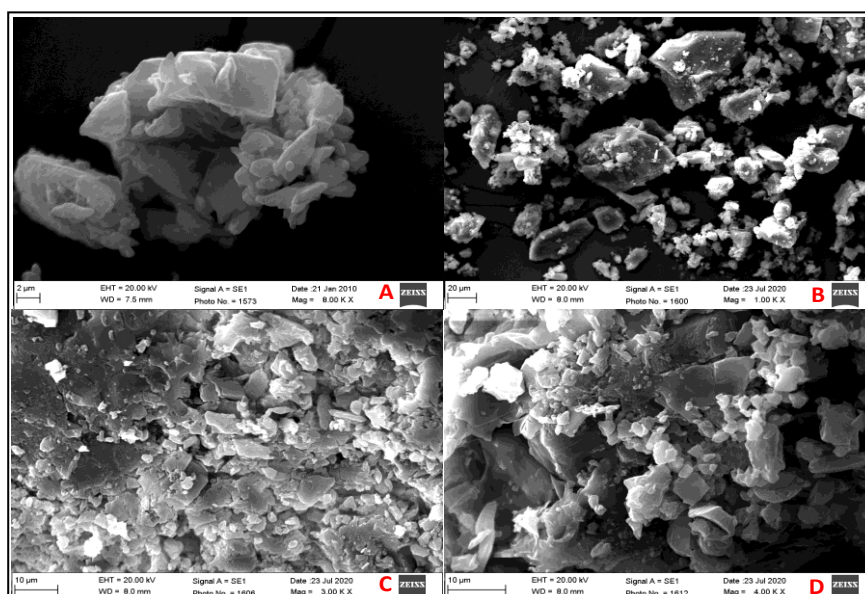


**Figure 5.** SEM images of (A) pure piperine, (B) piperine physical mixture, (C) piperine ternary inclusion complex (PPR TCM), (D) piperine ternary inclusion complex (PPR TCS).

### 3.5. Fourier Transform Infrared (FTIR)

The ascribed IR vibrations of the pure piperine (PPR), carriers beta cyclodextrin ( $\beta$  CD), and hydroxy propyl methylcellulose (HPMC) were performed compared with the prepared formulations (PPR TPM, PPR TCM, and PPR TCS). The characteristic functional groups accountable for being congruous with stretching frequencies are represented in Figure 6. PPR is an alkaloid, belonging to the family of nitrogenous compounds, it exhibited a sharp stretching spectral peak for tertiary nitrogen at  $2938.12\text{ cm}^{-1}$ . The characteristic carbonyl stretching vibrations were observed at  $1631.17\text{ cm}^{-1}$ . The C–O–C, C=C ethylenic, and C=C aromatic stretching peaks were also observed at  $1151.28$ ,  $1561.82$ , and  $1442.31\text{ cm}^{-1}$  for the pure PPR, respectively [32]. The featured frequencies for  $\beta$  CD were recognized at  $3277.42$  and  $1149.51\text{ cm}^{-1}$ , which contemplate the stretching vibration of O–H and C–O–C moiety. The carrier also established a peak for the  $\text{CH}_2$  bending vibration at  $1413.18\text{ cm}^{-1}$ . The most perceptible peak for HPMC was the stretching vibration at  $1048.40\text{ cm}^{-1}$  for the C–O–C group. Hydroxy propyl (CH–OH) peaks of methyl cellulose were visible at  $3350.18\text{ cm}^{-1}$ , whereas the C–OH in-plane bending vibration of cellulose was observed at  $1450.12\text{ cm}^{-1}$ .

Piperine ternary physical mixture (PPR TPM) and ternary inclusion complexes (PPR TCS and PPR TCM) showed the presence of a tertiary nitrogen peak ( $\text{CH}_2\text{–N}$ ) of PPR, which was also confirmed by  $^1\text{H}$  NMR, with a slight variation at  $2930.12$ ,  $2930.16$ , and  $2931.12\text{ cm}^{-1}$ , respectively. There was a drastic variation in the peaks for C=C aromatic having vibrations at  $1437.28\text{ cm}^{-1}$  for TPM,  $1439.92$  for TCM, and  $1441.86$  for PPR TCS. The substantial change was also observed for C–O–C stretching, which corresponded to  $1025.13$ ,  $1025.95$ , and  $1024.75\text{ cm}^{-1}$ , respectively. The above radical change for C=C aromatic and C–O–C stretching might be imputed to the occupancy of carriers. Further, C=C ethylenic stretching vibrations were observed at  $1568.43\text{ cm}^{-1}$  for PPR TPM, PPR TCM, and PPR TCS. The peaks for carbonyl moiety (C=O) of the pure PPR were also observed at  $1632.26\text{ cm}^{-1}$  in the complexes PPR TPM, PPR TCM, and PPR TCS. The complexes PPR TPM and PPR TCS also showed broad peaks of hydroxyl moiety at  $3281.17\text{ cm}^{-1}$  of the  $\beta$  CD carrier, whereas PPR TCM showed the hydroxyl peaks of the carrier HPMC at  $3318.93\text{ cm}^{-1}$ , which is in compliance with the proton NMR. It may be presumed due to the complexation of PPR with carriers.

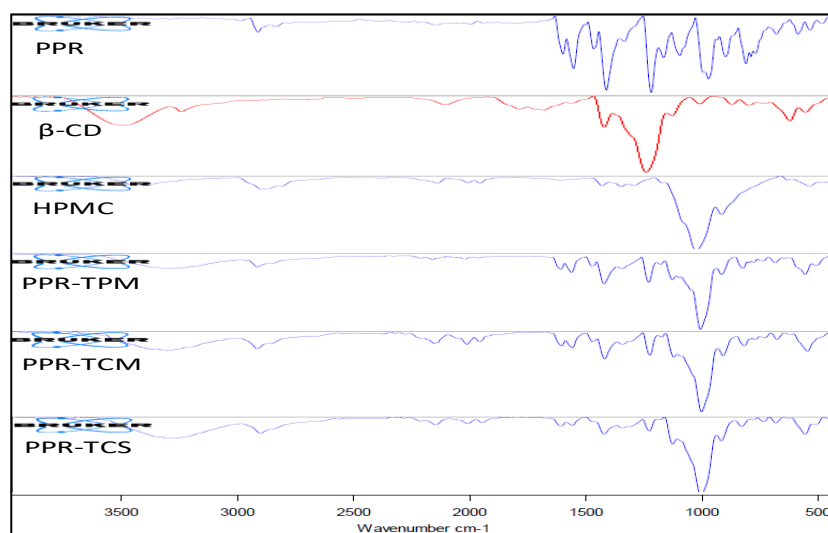


**Figure 6.** IR spectra of pure samples (piperine,  $\beta$  CD, HPMC), prepared formulations (piperine physical mixture, piperine ternary inclusion complex (PPR TCM), piperine ternary inclusion complex (PPR TCS).

### 3.6. Nuclear Magnetic Resonance (NMR)

$^1\text{H}$  and  $^{13}\text{C}$  NMR of pure PPR, PPR TPM, PPR TCM, and PPR TCS were performed to explore the relations connecting pure PPR and carriers ( $\beta$  CD and HPMC) utilizing the chemical shift ( $\delta$ ), as shown in Figures 7 and 8. The chemical shift values of proton NMR spectra of pure PPR (Figure 7),

were collated with the formed complexes of PPR TPM, PPR TCM, and PPR TCS. The proton NMR spectrum of PPR in DMSO-d<sub>6</sub> showed a distinct singlet at 6.03 ppm, which was attributed to the methylenic proton of benzodioxole. The multiplet peak was observed for the piperidine ring at C-3, C-4, and C-5 having  $\delta$  value of 1.50–1.61 ppm. The singlet CH<sub>2</sub>-N peak for the piperidine ring was also observed at  $\delta$  3.52 ppm. The structure also exhibited multiplet peaks of benzene at  $\delta$  value of 6.87–6.99 ppm. Two distinct peaks for ethylene at position 2' and 4' having a sharp singlet peak were also seen at  $\delta$  6.62 and 7.24 ppm. The singlet peaks at 3' and 5' of the ethylenic bond were observed at  $\delta$  7.18 and 6.65 ppm. The singlet peak for the  $\beta$  CD carrier was explored at  $\delta$  5.76 ppm at position 1 of the glucose moiety. The singlet peak of hydroxyl moiety of the carrier was seen at  $\delta$  2.40 ppm. Chemical shift values of the second carrier HPMC showed a singlet methoxy (-OCH<sub>3</sub>) peak at  $\delta$  3.11. The distinct singlet CH peaks of hydroxyl propyl (CH-OH) were visible at  $\delta$  3.72, whereas the hydroxyl (C-OH) peak of cellulose was observed at  $\delta$  2.00 ppm. The methylene (-CH<sub>2</sub>) and free methyl moiety (-CH<sub>3</sub>) of hydroxyl propyl (CH<sub>2</sub>-CHOH-CH<sub>3</sub>) of the carrier were observed at  $\delta$  3.52 and  $\delta$  1.21 ppm, respectively. In disparity, the complexes PPR TPM, PPR TCM, and PPR TCS depicted totally imperceptible changes in the  $\delta$  values of methylene moiety of benzodioxole with a singlet  $\delta$  value of 6.04 ppm. A minor change was observed for the multiplet peaks of the piperidine ring at C-3, C-4, and C-5 having  $\delta$  value of 1.50–1.62 ppm for the formed complexes PPR TPM, PPR TCM, and PPR TCS. The singlet CH<sub>2</sub>-N peak of the piperidine ring was also observed at  $\delta$  3.55 ppm for the complexes as in compliance with IR spectral values. The PPR TPM and the inclusion complex (PPR TCM and PPR TCS) almost exhibited a similar multiplet peak of benzene with a slight change at  $\delta$  value of 6.91–6.97 ppm. The two distinct singlet peaks for ethylene at position 2' and 4' were seen at  $\delta$  6.68 and 7.19 ppm and at position 3' and 5' were observed at  $\delta$  7.21 and 6.71 ppm for the complexes PPR TPM, PPR TCM, and PPR TCS. The carrier peaks of  $\beta$  CD glucose at  $\delta$  5.74 ppm were also observed in all the complexes with minor changes in chemical shift values, which may indicate the formation of complexes. All the complexes exhibited the value of  $\delta$  1.47 ppm for the free methyl group (CH<sub>2</sub>-CHOH-CH<sub>3</sub>) of HPMC. The singlet hydroxyl peak of the carrier  $\beta$  CD was also observed in the complexes PPR TPM and PPR TCS at  $\delta$  2.43 ppm but PPR TCM observed hydroxyl peaks at  $\delta$  2.01 ppm peaks, which was the singlet hydroxyl peak of the carrier HPMC, as in compliance with the IR spectral value. The results of proton NMR and IR spectral values of PPR TCM showed that the  $\beta$  CD and HPMC peaks encountered massive adjustment, which exhibited its gravity in the solubility augmentation of PPR. The appearance of the carbonyl group of pure PPR and the hydroxyl group of the carriers in complexes with minute chemical shift also stipulate the formation of complexes. The significant upfield shift in presence of  $\beta$  CD was observed for aromatic protons of PPR.

In <sup>13</sup>C NMR (Figure 8), a slight deviation was observed for PPR TPM, PPR-TCM, and PPR-TCS for piperidine ring in all the complexes at  $\delta$  value of 46.56 at C-2,6,  $\delta$  26.94 at C-3,5, and  $\delta$  24.61 ppm at C-4 position. For the pure PPR, the  $\delta$  value of piperidine ring was found to be at 46.51 ppm for C-2, 26.91 ppm for C-3, 5 and 24.66 ppm for C-4 position. The aforementioned result was in compliance with <sup>1</sup>H and IR spectroscopy. The benzodioxole ring of the pure PPR showed the presence of  $\delta$  value at 101.74 ppm, whereas the complexes showed slight shifting in  $\delta$  values at 101.77 ppm. The presence of glucopyranoside peaks of the carrier  $\beta$  CD in complexes was found to be at  $\delta$  82.96 ppm as compared to the carrier peaks of which was found to be at  $\delta$  82.93 ppm. The complexes also showed a distinct slight shift in peaks for the carrier HPMC at  $\delta$  72.53 ppm for CH-OH which was at  $\delta$  72.51 ppm originally for the carrier. The extra peaks were also observed which may be due to the carriers indicating the formation of complexes. The above spectroscopic values reassured that the interaction between the pure PPR and carriers leads to the formation of complexes. The spectral IR and NMR values also confirmed that the complex PPR TCM showed the significant solubility enhancement in presence of the carriers. The above statement is concluded on the basis of the explanation given by the various spectral characteristic values which is further supported by molecular docking studies.

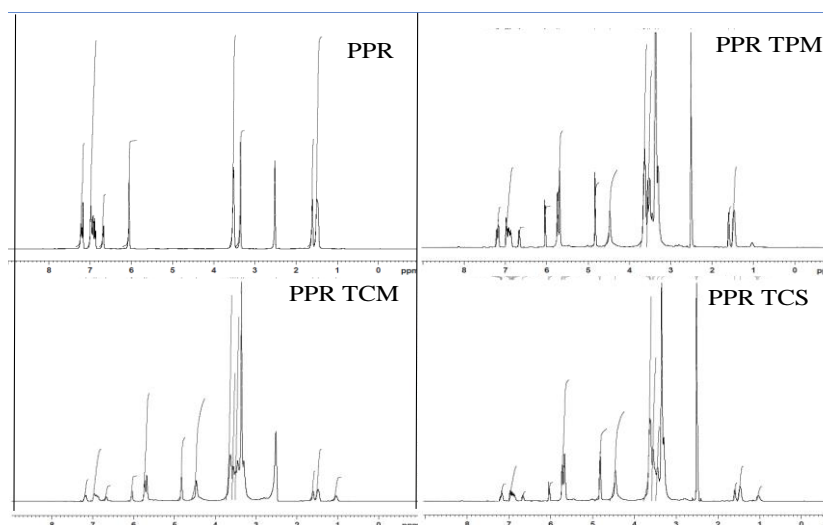


**Figure 7.**  $^1\text{H}$  spectra of pure piperine (PPR), piperine physical mixture (PPR TPM), piperine ternary inclusion complex, (D) piperine ternary inclusion complex (PPR TCS).

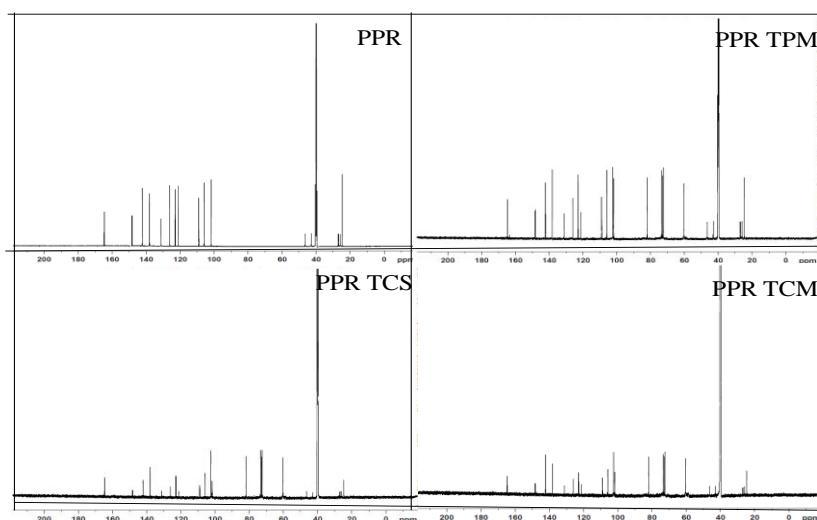


**Figure 8.**  $^{13}\text{C}$  spectra of pure piperine, piperine physical mixture, piperine ternary inclusion complex (PPR TCM), piperine ternary inclusion complex (PPR TCS).

### 3.7. Antioxidant Activity

The antioxidant activity of the prepared samples was assessed by the DPPH method [20]. The antioxidant molecule has the property to react with the proton donor group and converts to violet color. The antioxidant activity of all the samples was performed at fixed concentration of 100  $\mu\text{g}/\text{mL}$  (PPR). The pure PPR showed the maximum activity of  $38.92 \pm 2.38\%$ , whereas the prepared samples showed higher antioxidant property. PPR TPM, PPR TCS, and PPR TCM showed the maximum activity of  $59.42 \pm 4.1\%$ ,  $72.37 \pm 5.35\%$ , and  $79.19 \pm 4.34\%$ , respectively (Table 2). The study results indicated a significant ( $p < 0.01$ ) enhancement in activity in the inclusion complex formulation as compared to pure PPR. The antioxidant activity of piperine has been reported in our previous study and result showed 42.27% at 100  $\mu\text{g}/\text{mL}$  concentration [23]. In this study, PPR TCM (100  $\mu\text{g}/\text{mL}$ ) depicted significantly 1.87 fold higher activity at the same concentration. In the DPPH radical scavenging reaction, conversion of DPPH-H takes place from DPPH due to the reason of antioxidant donating the hydrogen or electron. The antioxidant activity mainly depends on the electron or hydrogen donating property [9,33,34]. The formation of different PPR samples with CD and HPMC (PPR TPM, PPR TCS, and PPR TCM), the scavenging activity enhanced due to increased free radicals [35] and solubility.

### 3.8. Antimicrobial Activity

The antimicrobial activity of the prepared samples was evaluated against the different microorganisms and results were compared with the pure PPR (Figure 9 and Table 2). The pure PPR showed the ZOI as  $11.4 \pm 0.45$  mm,  $9.3 \pm 0.38$  mm,  $11.8 \pm 0.65$  mm, and  $6.9 \pm 0.53$  mm against *S. aureus*, *B. subtilis*, *E. coli*, and *E. faecalis*, respectively. The prepared samples PPR TCM and PPR TCS showed enhanced antibacterial activity against all the tested organisms. The enhanced ZOI result was found for PPR TCM as  $15.7 \pm 0.73$  mm,  $12.9 \pm 0.79$  mm,  $16.2 \pm 0.82$  mm, and  $11.9 \pm 0.53$  mm against *S. aureus*, *B. subtilis*, *E. coli*, and *E. faecalis*, respectively. The PPR TCS treated organism also showed the result closer to PPR TCM treated ZOI. The ZOI of PPR TCS treated organisms showed  $15.5 \pm 0.89$  mm,  $13.1 \pm 0.72$  mm,  $16.5 \pm 0.66$  mm, and  $11.3 \pm 0.85$  mm against *S. aureus*, *B. subtilis*, *E. coli*, and *E. faecalis*, respectively. From the result, it was observed that the prepared ternary complexes (PPR TCS and PPR TCM) are highly sensitive against Gram-negative bacterial (*E. coli*). The results of the study showed marked effect against *S. aureus*, *B. subtilis*. The enhanced antibacterial achieved may be due to the presence of phenolic and flavonoid nature of PPR. The greater activity of the PPR complex due to the enhanced solubility of PPR after complexation with  $\beta$  CD and HPMC. It has been also reported that, CDs can enhance the antimicrobial property by increasing the solubility and release rate from the inclusion complex [23,36].

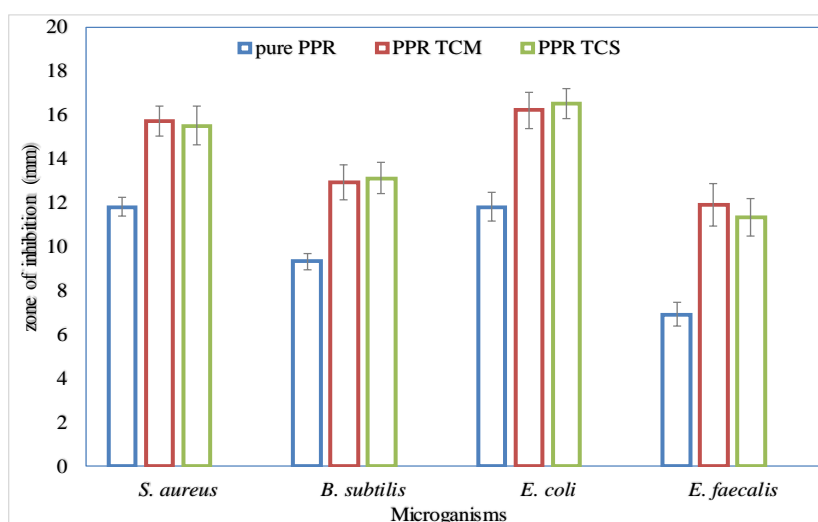


**Figure 9.** Comparative antimicrobial study results against different micro-organisms [(ZOI noted after subtracting the value of well 6 mm)].

### 3.9. Molecular Docking

In our effort to understand the stable molecular arrangement in the inclusion complexes, we focused on the molecular interactions of PPR and HPMC with  $\beta$  CD. Auto Dock 4.2 with a Lamarckian genetic algorithm-implemented program suite was employed to identify appropriate binding modes and conformation of the ligand molecules. The docked conformations of the two ligands PPR and HPMC bound to  $\beta$  CD are shown in Figure 10A,B. The docking studies have revealed that the binding affinity of PPR at the  $\beta$  CD was  $-5.2$  kcal/mol. The binding interaction of ternary inclusion complex revealed that PPR and HPMC were aligned in the central cavity of  $\beta$  CD. The benzodioxolyl ring occupied the  $\beta$  CD cavity, whereas the terminal piperidine ring protruded out of the cavity for PPR (Figure 10A). The aromatic benzodioxolyl ring of PPR occupied the hydrophobic portion inside the  $\beta$  CD. The ternary inclusion complex of PPR,  $\beta$  CD, and HPMC was modeled by docking HPMC on the binary inclusion complex of PPR and  $\beta$  CD. The docking studies have revealed that the binding affinity of HPMC at the PPR- $\beta$  CD complex was  $-4.7$  kcal/mol. The molecular interaction studies of HPMC showed that the (1,4)-beta-D-glucan moiety occupied the central cavity of the  $\beta$  CD, whereas the aliphatic hydroxypropyl side chain remained outside the  $\beta$  CD (Figure 10B). No steric hindrance was observed

between PPR and HPMC molecules when put together inside the  $\beta$  CD cavity, hence the prepared ternary inclusion system might be considered as thermodynamically stable.

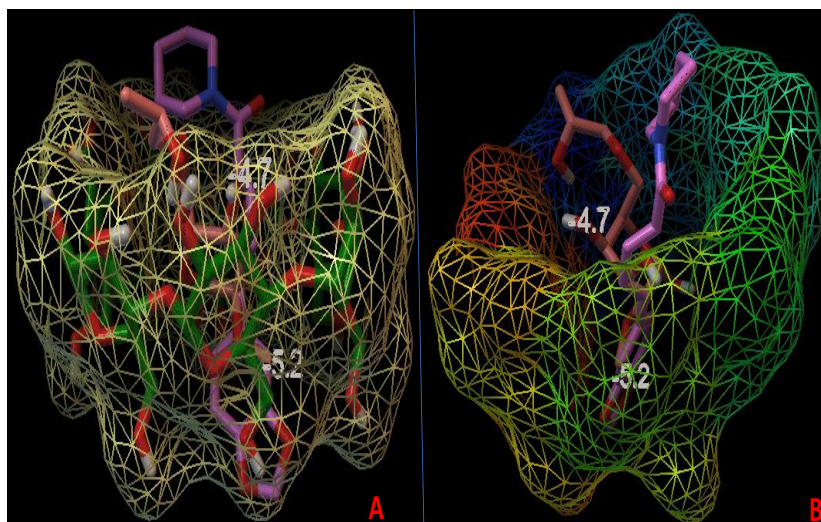


**Figure 10.** (A) The side binding poses of the piperine ternary inclusion complex [Ball and stick model of piperine (grey color) and HPMC (orange color)  $\beta$  CD (wire and mesh), (B) binding mode of PPR, HPMC at the central cavity of  $\beta$  CD (top view).

#### 4. Conclusions

In this study, PPR- $\beta$  CD-HPMC inclusion complex was prepared by solvent evaporation and the microwave irradiation method. The samples showed the stability constant result in the optimum range. The dissolution study results showed significant enhancement in the drug release profile. The solid state characterization results reported the formation of the complex with the presence of more agglomerated and amorphous PPR structure. The NMR spectroscopic and molecular docking results also confirmed the formation of the inclusion complex between the pure PPR and carriers. DPPH radical scavenging and antimicrobial activity results revealed a significant ( $p < 0.05$ ) enhancement in the activity. The geometry of the complex showed that, the aromatic benzodioxolyl ring of PPR occupied inside the  $\beta$  CD and (1,4)-beta-D-glucan moiety of HPMC occupied the central cavity of the  $\beta$  CD, whereas the aliphatic hydroxypropyl side chain remained outside the  $\beta$  CD. The enhancement in results was achieved due to the marked enhancement in the solubility of the insoluble PPR.

**Author Contributions:** Conceptualization, S.S.I., and S.A.; methodology, S.S.I.; data curation, S.S.I.; software, S.S.I.; writing—original draft, S.S.I.; resources, S.A; writing—review & editing, S.A., A.H., and M.A.A.; funding acquisition, S.A. All authors have read and agreed to the published version of the manuscript.

**Funding:** The research was funded by the Deputyship for Research & Innovation, “Ministry of Education” in Saudi Arabia for funding this research work through the project number IFKSURG-145.

**Acknowledgments:** The authors extend their appreciation to the Deputyship for Research & Innovation, “Ministry of Education” in Saudi Arabia for funding this research work through the project number IFKSURG-145.

**Conflicts of Interest:** The authors declare no conflict of interest.

#### References

1. Kurup, M.P.; Nirmal, C.R.; Dusthacker, A.; Magizhaveni, B.; Kurup, M.R.P.; Balasubramanian, M. Formulation and evaluation of  $\beta$ -cyclodextrin-mediated inclusion complexes of isoniazid scaffolds: Molecular docking and in vitro assessment of antitubercular properties. *New J. Chem.* **2020**, *44*, 4467–4477. [[CrossRef](#)]
2. Qiu, N.; Zhao, X.; Liu, Q.; Shen, B.; Liu, J.; Li, X.; An, L. Inclusion complex of emodin with hydroxypropyl- $\beta$ -cyclodextrin: Preparation, physicochemical and biological properties. *J. Mol. Liq.* **2019**, *289*, 111151. [[CrossRef](#)]

3. Gao, S.; Bie, C.; Ji, Q.; Ling, H.; Li, C.; Fu, Y.; Zhao, L.; Ye, F. Preparation and characterization of cyanazine–hydroxypropyl-beta-cyclodextrin inclusion complex. *RSC Adv.* **2019**, *9*, 26109–26115. [[CrossRef](#)]
4. Mohandoss, S.; Atchudan, R.; Edison, T.N.J.I.; Mandal, T.K.; Palanisamy, S.; You, S.; Napoleon, A.A.; Shim, J.-J.; Lee, Y.R. Enhanced solubility of guanosine by inclusion complexes with cyclodextrin derivatives: Preparation, characterization, and evaluation. *Carbohydr. Polym.* **2019**, *224*, 115166. [[CrossRef](#)]
5. Kurkov, S.V.; Loftsson, T. Cyclodextrins. *Int. J. Pharm.* **2013**, *453*, 167–180. [[CrossRef](#)]
6. Ren, T.; Hu, M.; Cheng, Y.; Shek, T.L.; Xiao, M.; Ho, N.J.; Zhang, C.; Leung, S.S.Y.; Zuo, Z. Piperine-loaded nanoparticles with enhanced dissolution and oral bioavailability for epilepsy control. *Eur. J. Pharm. Sci.* **2019**, *137*, 104988. [[CrossRef](#)]
7. Liu, G.; Yuan, Q.-J.; Hollett, G.; Zhao, W.; Kang, Y.; Wu, J. Cyclodextrin-based host–guest supramolecular hydrogel and its application in biomedical fields. *Polym. Chem.* **2018**, *9*, 3436–3449. [[CrossRef](#)]
8. Ding, X.; Zheng, M.; Lu, J.; Zhu, X. Preparation and evaluation of binary and ternary inclusion complexes of fenofibrate/hydroxypropyl- $\beta$ -cyclodextrin. *J. Incl. Phenom. Macrocycl. Chem.* **2018**, *91*, 17–24. [[CrossRef](#)]
9. AlShehri, S.; Imam, S.S.; Altamimi, M.A.; Jafar, M.; Hassan, M.Z.; Hussain, A.; Ahad, A.; Mahdi, W. Host-guest complex of  $\beta$ -cyclodextrin and pluronic F127 with Luteolin: Physicochemical characterization, anti-oxidant activity and molecular modeling studies. *J. Drug Deliv. Sci. Technol.* **2020**, *55*, 101356. [[CrossRef](#)]
10. Mourão, L.C.D.S.; Batista, D.R.M.R.; Honorato, S.B.; Ayala, A.P.; Morais, W.D.A.; Barbosa, E.G.; Raffin, F.N.; Moura, T. Effect of hydroxypropyl methylcellulose on beta cyclodextrin complexation of praziquantel in solution and in solid state. *J. Incl. Phenom. Macrocycl. Chem.* **2016**, *85*, 151–160. [[CrossRef](#)]
11. Mohanty, B.; Suvitha, A.; Venkataramanan, N.S. Piperine Encapsulation within Cucurbit[n]uril (n = 6, 7): A Combined Experimental and Density Functional Study. *Chem.* **2018**, *3*, 1933–1941. [[CrossRef](#)]
12. Quilaqueo, M.; Millao, S.; Luzardo-Ocampo, I.; Campos-Vega, R.; Acevedo, F.; Shene, C.; Rubilar, M. Inclusion of piperine in  $\beta$ -cyclodextrin complexes improves their bioaccessibility and in vitro antioxidant capacity. *Food Hydrocoll.* **2019**, *91*, 143–152. [[CrossRef](#)]
13. Ezawa, T.; Inoue, Y.; Tunvichien, S.; Suzuki, R.; Kanamoto, I. Changes in the Physicochemical Properties of Piperine/ $\beta$ -Cyclodextrin due to the Formation of Inclusion Complexes. *Int. J. Med. Chem.* **2016**, *2016*, 1–9. [[CrossRef](#)]
14. Karsha, P.V.; Lakshmi, O.B. Antibacterial activity of black pepper (*Piper nigrum* Linn.) with special reference to its mode of action on bacteria. *Indian J. Nat. Prod. Resour.* **2010**, *1*, 213–215.
15. Anissian, D.; Ghasemi-Kasman, M.; Khalili-Fomeshi, M.; Akbari, A.; Hashemian, M.; Kazemi, S.; Akbar Moghadamnia, A. Piperine-loaded chitosan-STPP nanoparticles reduce mortal neuronal loss and astrocytes activation in chemical kindling model of epilepsy. *Int. J. Biol. Macromol.* **2018**, *107*, 973–983. [[CrossRef](#)]
16. Higuchi, T.; Connors, K.A. Phase solubility techniques. *Adv. Anal. Chem. Instrum.* **1965**, *4*, 117–122.
17. Loh, G.O.K.; Tan, Y.T.F.; Peh, K.K. Effect of HPMC concentration on  $\beta$ -cyclodextrin solubilization of norfloxacin. *Carbohydr. Polym.* **2014**, *101*, 505–510. [[CrossRef](#)]
18. Patel, M.; Hirlekar, R. Multicomponent cyclodextrin system for improvement of solubility and dissolution rate of poorly water soluble drug. *Asian J. Pharm. Sci.* **2019**, *14*, 104–115. [[CrossRef](#)]
19. Khajuria, A.; Zutshi, U.; Bedi, K.L. Permeability characteristics of piperine on oral absorption—an active alkaloid from peppers and a bioavailability enhancer. *Indian J. Exp. Biol.* **1998**, *36*, 46–50.
20. Zarai, Z.; Boujelbene, E.; Ben Salem, N.; Gargouri, Y.; Sayari, A. Antioxidant and antimicrobial activities of various solvent extracts, piperine and piperic acid from *Piper nigrum*. *LWT* **2013**, *50*, 634–641. [[CrossRef](#)]
21. Adachi, M.; Mikami, B.; Katsube, T.; Utsumi, S. Crystal Structure of Recombinant Soybean  $\beta$ -Amylase Complexed with  $\beta$ -Cyclodextrin. *J. Biol. Chem.* **1998**, *273*, 19859–19865. [[CrossRef](#)] [[PubMed](#)]
22. De Freitas, M.R.; Rolim, L.A.; Soares, M.F.D.L.R.; Rolim-Neto, P.J.; De Albuquerque, M.M.; Soares-Sobrinho, J.L. Inclusion complex of methyl- $\beta$ -cyclodextrin and olanzapine as potential drug delivery system for schizophrenia. *Carbohydr. Polym.* **2012**, *89*, 1095–1100. [[CrossRef](#)] [[PubMed](#)]
23. Imam, S.S.; AlShehri, S.M.; Alzahrani, T.A.; Altamimi, M.A.; Altamimi, M.A. Formulation and Evaluation of Supramolecular Food-Grade Piperine HP  $\beta$  CD and TPGS Complex: Dissolution, Physicochemical Characterization, Molecular Docking, In Vitro Antioxidant Activity, and Antimicrobial Assessment. *Molecules* **2020**, *25*, 4716. [[CrossRef](#)] [[PubMed](#)]
24. Hirlekar, R.; Sonawane, S.N.; Kadam, V.J. Studies on the Effect of Water-Soluble Polymers on Drug–Cyclodextrin Complex Solubility. *AAPS PharmSciTech* **2009**, *10*, 858–863. [[CrossRef](#)]

25. Suvarna, V.; Kajwe, A.; Murahari, M.; Pujar, G.V.; Inturi, B.K.; Sherje, A.P. Inclusion Complexes of Nateglinide with HP- $\beta$ -CD and L-Arginine for Solubility and Dissolution Enhancement: Preparation, Characterization, and Molecular Docking Study. *J. Pharm. Innov.* **2017**, *12*, 168–181. [[CrossRef](#)]
26. AlShehri, S.M.; Imam, S.S.; Altamimi, M.A.; Hussain, A.; Shakeel, F.; AlShehri, A. Stimulatory Effects of Soluplus<sup>®</sup> on Flufenamic Acid  $\beta$ -Cyclodextrin Supramolecular Complex: Physicochemical Characterization and Pre-clinical Anti-inflammatory Assessment. *AAPS PharmSciTech* **2020**, *21*, 1–13. [[CrossRef](#)]
27. Nogueiras-Nieto, L.; Sobarzo-Sánchez, E.; Espinar, F.J.O.; Otero-Espinar, F.J. Competitive displacement of drugs from cyclodextrin inclusion complex by polypseudorotaxane formation with poloxamer: Implications in drug solubilization and delivery. *Eur. J. Pharm. Biopharm.* **2012**, *80*, 585–595. [[CrossRef](#)] [[PubMed](#)]
28. AlShehri, S.M.; Imam, S.S.; Altamimi, M.A.; Hussain, A.; Shakeel, F.; Elzayat, E.M.; Mohsin, K.; Ibrahim, M.; Alanazi, F. Enhanced Dissolution of Luteolin by Solid Dispersion Prepared by Different Methods: Physicochemical Characterization and Antioxidant Activity. *ACS Omega* **2020**, *5*, 6461–6471. [[CrossRef](#)]
29. Zawar, L.R.; Bari, S.B. Preparation, Characterization and in Vivo Evaluation of Antihyperglycemic Activity of Microwave Generated Repaglinide Solid Dispersion. *Chem. Pharm. Bull.* **2012**, *60*, 482–487. [[CrossRef](#)]
30. Sami, F.; Philip, B.; Pathak, K. Effect of auxiliary substances on complexation efficiency and intrinsic dissolution rate of gemfibrozil- $\beta$ -CD complexes. *AAPS PharmSciTech* **2010**, *11*, 27–35. [[CrossRef](#)]
31. Bera, H.; Chekuri, S.; Sarkar, S.; Kumar, S.; Muvva, N.B.; Mothe, S.; Nadimpalli, J. Novel pimozone- $\beta$ -cyclodextrin-polyvinylpyrrolidone inclusion complexes for Tourette syndrome treatment. *J. Mol. Liq.* **2016**, *215*, 135–143. [[CrossRef](#)]
32. Ren, Z.; Xu, Y.; Lu, Z.; Wang, Z.; Chen, C.; Guo, Y.; Shi, X.; Li, F.; Yang, J.; Zheng, Y. Construction of a water-soluble and photostable rubropunctatin/ $\beta$ -cyclodextrin drug carrier. *RSC Adv.* **2019**, *9*, 11396–11405. [[CrossRef](#)]
33. Shirwaikar, A.; Shirwaikar, A.; Rajendran, K.; Punitha, I.S.R. In Vitro Antioxidant Studies on the Benzyl Tetra Isoquinoline Alkaloid Berberine. *Biol. Pharm. Bull.* **2006**, *29*, 1906–1910. [[CrossRef](#)] [[PubMed](#)]
34. Mohamed, H.; Jarraya, R.; Lassoued, I.; Masmoudi, O.; Damak, M.; Nasri, M. GC/MS and LC/MS analysis, and antioxidant and antimicrobial activities of various solvent extracts from *Mirabilis jalapa* tubers. *Process. Biochem.* **2010**, *45*, 1486–1493. [[CrossRef](#)]
35. Soni, K.; Rizwanullah; Kohli, K. Development and optimization of sulforaphane-loaded nanostructured lipid carriers by the Box-Behnken design for improved oral efficacy against cancer: In vitro, ex vivo and in vivo assessments. *Artif. Cells Nanomed. Biotechnol.* **2018**, *46*, 15–31. [[CrossRef](#)]
36. Aleem, O.; Kuchekar, B.; Pore, Y.; Late, S. Effect of  $\beta$ -cyclodextrin and hydroxypropyl  $\beta$ -cyclodextrin complexation on physicochemical properties and antimicrobial activity of cefdinir. *J. Pharm. Biomed. Anal.* **2008**, *47*, 535–540. [[CrossRef](#)]

**Publisher's Note:** MDPI stays neutral with regard to jurisdictional claims in published maps and institutional affiliations.



© 2020 by the authors. Licensee MDPI, Basel, Switzerland. This article is an open access article distributed under the terms and conditions of the Creative Commons Attribution (CC BY) license (<http://creativecommons.org/licenses/by/4.0/>).